NASA
Technical Memorandum 82877

AVRADCOM
Technical Report 82-C-12

Comparison of Experimental and Analytic Performance for Contoured Endwall Stators

(NASA-TM-82877) COMPARISON OF EXPERIMENTAL AND ANALYTICAL PERFORMANCE FOR CONTOURED ENDWALL STATORS (NASA) 15 p HC A02/MF A01 CSCL 21E
N82-26299
Unclas
G3/07 28128

Robert J. Boyle
Lewis Research Center
Cleveland, Ohio

and

Jeffrey E. Haas
Propulsion Laboratory
AVRADCOM Research and Technology Laboratories
Lewis Research Center
Cleveland, Ohio

Prepared for the
Eighteenth Joint Propulsion Conference
cosponsored by the AIAA, SAE, and ASME
Cleveland, Ohio, June 21-23, 1982

NASA

E-1252

COMPARISON OF EXPERIMENTAL AND ANALYTIC PERFORMANCE FOR CONTOURED ENDWALL STATORS

Robert J. Boyle
National Aeronautics and Space Administration
Lewis Research Center
Cleveland, Ohio 44135

and

Jeffrey E. Haas
Propulsion Laboratory
AVRADCOM Research and Technology Laboratories
Lewis Research Center
Cleveland, Ohio 44135

Abstract

Comparisons between predicted and experimental stator losses showed that the analysis was able to predict the change in stator loss when contoured endwalls with highly three-dimensional passage geometry were used. The level of loss was predicted to within 75 percent of that measured. The predicted loss was due only to profile loss and boundary layer growth on the endwalls. The 25 percent difference was approximately 0.015 at design pressure ratio. The analysis was shown to predict the trend in stator flow angle, even for small stator geometries.

Summary

Comparisons were made between analytic results and experimental results for contoured endwall stators. The comparisons were made for flow angle and stator aerodynamic loss. The contoured stators had variable radius outer endwalls which resulted in highly three-dimensional passage geometries. The results of these comparisons showed that even though the flow analysis was only quasi-three-dimensional in nature, it was able to predict changes in flow angle caused by three dimensional passage geometry. An inviscid flow analysis was used, and losses were calculated by coupling a boundary layer analysis to the flow analysis. Even for small sized stators, the analysis was able to predict the change in stator performance resulting from changes in the endwall geometry. Except for a case with large unfavorable pressure gradients, the difference between the predicted and measured stator loss was less than 0.015. The difference of 0.015 corresponded to about 25 percent of the measured loss, so that the analysis was able to account for 75 percent of the measured loss. It was expected that the analysis would underpredict the experimental loss, since only analytic losses due to boundary layer growth and the presence of the trailing edge were accounted for. Endwall boundary layer loss was a large fraction of the total calculated loss.

Correlations were observed between calculated suction surface static pressures and experimental radial distribution of loss. For the cylindrical endwall stator there were high losses near the hub, and the minimum surface pressure on the blade occurred at the hub. For an S-contoured stator there was a high loss region near the tip, and the minimum suction surface pressure was also at the tip. For the conical stator the experimental data showed a high loss region near the tip, but the calculated minimum streamwise surface pressure varied little from hub to tip.

The choice of appropriate contour geometry is strongly influenced by blade loading. When unfavorable pressure gradients are reduced through contouring, significant reductions in stator loss are calculated. Calculations are presented to show the evolution of a contour design to give reduced loss and the desired amount of turning.

Introduction

A major goal of the turbine reseach program at the NASA-Lewis Research Center is to be able to predict the aerodynamic performance of turbine designs with complex passages. One type of complex passage which has received considerable attention is contoured endwall stators. In a contoured stator the tip radius varies with axial distance to form a highly three-dimensional nozzle. This application has received attention because contouring has the potential for reducing stator losses in two ways. First, the boundary layer growth is modified due to the lower velocity at the inlet and during most of the turning. Second, there is a reduction in secondary losses by virtue of the reduced pressure gradient both across the channel and in the radial direction. The low velocity turning resulting from contouring reduces the cross channel pressure gradient, and contouring the outer wall reduces the radial pressure gradient. Reducing the boundary layer growth increases stator efficiency, and reduced pressure gradients can yield more predictable rotor inlet conditions to improve stage efficiency.

There have been several studies giving the performance results for contoured endwalls. References 1 through 8 reported experimental investigations that showed improved performance due to endwall contouring. An analytic and experimental program was conducted at NASA-Lewis to investigate stator endwall contouring. The results of this program were reported in Refs. 9 and 10. One of the goals of this program was to see how well a quasi-three-dimensional flow analysis program could be used to predict the reduction in stator loss due to contouring.

The results presented herein include comparisons of the analysis with the experimental results of Refs. 7, 8, and 10. The analysis is compared with data from different sources to show its ability to predict performance results for different geometries and blade loadings. Reference 7 gives surface pressures and flow angles for a single contoured endwall stator. References 8 and 10 each give experimental loss values for three stators. In each program the performance of two contoured stators were compared with a cylindrical endwall case. The stators of Ref. 8 were more highly loaded than those of Refs. 10. Comparisons are made between analytic and experimental flow angles and stator losses. The effect of contouring on stator loss is discussed, along with an illustration of the evolution of a contour geometry to give low stator loss. Also, the effect of Reynolds number on loss reduction due to contouring is discussed.

The analysis used the quasi-three-dimensional flow analysis of Refs. 11 and 12 to calculate blade and endwall surface velocities. In addition, a boundary layer analysis[13] was used to determine properties for use in profile and endwall loss models. The profile loss model of Ref. 14 was used, and the endwall loss model is described in Appendix A.

Method of Analysis

Figure 1 shows the geometry of a contoured endwall configuration. This figure shows a blade passage bounded by two blades, a cylindrical hub, and a contoured tip. The tip contour is axi-symmetric rather than being aligned with the direction of the flow. In the three dimensional sketch the contour appears to be fairly shallow. This is the result of the large amount of turning in the passage. The projection shows a rapid change in endwall radius in the last half of the chord. The analysis was done by specifying conditions upstream of the blade and also the whirl a distance downstream of the trailing edge. The whirl varied with radius.

An iterative procedure was used to determine stator performance. In the iterative procedure an initial estimate was made for the downstream whirl. With this estimate the flow field velocity distribution was determined using a quasi-three-dimensional inviscid analysis. Once the velocity distribution was found a boundary layer analysis was done to determine boundary layer thicknesses on both the blade surfaces and endwalls. A check was made of the static pressure difference across the blade near the trailing edge. When this difference did not approach zero, the estimate of the downstream whirl distribution was changed, and the procedure repeated.

The quasi-three-dimensional flow analysis was accomplished using two flow programs. Each program analyzes the flow on a single surface. The first program, MERIDL[11] calculates flow properties on the hub-shroud midchannel stream surface. One of the results of this program is the streamsheet thickness necessary to pass one percent of the total flow on a blade-to-blade surface of revolution. The thickness varied as a function of radius and axial distance. The calculated thicknesses were used as part of the input to the second flow analysis program. This program, TSONIC[12] calculates flow properties on blade-to-blade surfaces. Typically, the surfaces were the hub, tip, and three additional streamlines within the passage. The analysis was not fully three dimensional. This was because the stream sheet thickness necessary to pass one percent of the flow could not vary in the blade-to-blade direction, and all surfaces on which the blade-to-blade analysis was done were surfaces of revolution. When there was a significant supersonic region in the flow, a version of the TSONIC code was used which incorporated the modifications described in Ref. 15.

The inviscid surface velocities were used in a boundary layer analysis to calculate displacement and momentum thicknesses for both blade surface and endwall streamlines. This boundary layer analysis assumed turbulent compressible flow and was done using the program BLAYER described in Ref. 13. The boundary layer calculations were done for each iteration. The iteration procedure was stopped when the static pressures on each side of the blade were approximately equal near the trailing edge. The boundary layer analysis provided information regarding the uncertainty in the losses as the iterations progressed. Generally, several iterations were required. The change in the static pressure difference was small for the final few iterations. Since the stator loss was proportional to the momentum thickness near the trailing edge, the variation in momentum thickness for the last few iterations gave an estimate of the uncertainty in stator loss.

The total calculated loss for each case was taken as the sum of the profile loss and endwall loss. The profile loss was calculated using the procedure described in Ref. 14 for calculating the aftermixed efficiency based on kinetic energy. This procedure involved integration in the radial direction. At each radius the required information was obtained using the analysis given in Ref. 16 to determine mixed out losses. The endwall boundary layers were calculated to the axial location of the experimental measuring plane downstream of the stator. The method of calculating the endwall loss is analogous to that given in Ref. 16. Details are given in Appendix A.

Results and Discussion

Stator performance results from three sources with highly three dimensional passage geometries will be compared with the analysis. This is done to show the ability of the analysis to predict the change in stator performance due to changes in endwall geometry. Table I gives dimensional characteristics for the stators investigated. The stator tip diameters varied from 13 to 73 cm. The stators are referred to in the following discussion by their labels, which are descriptions of the tip endwall contours.

Comparison With the Experimental Data of Ref. 7

Figures 2(a) and (b) show calculated hub, mean, and tip blade inviscid surface velocities for a cylindrical and contoured tip endwall stator. This stator had an exit tip diameter of 73 cm, and an axial aspect ratio of 1.2 at the stator exit. Figure 2(a) shows a noticable amount of diffusion on the suction surface in the midspan to tip region for the cylindrical endwall case. Figure 2(b) shows that using a contoured endwall virtually eliminates this diffusion. Consequently, the boundary layer growth is less, but because of the large aspect ratio the calculated improvement in stator efficiency was only 0.003 for the contoured endwall case. Also shown in Fig. 2(a) are experimental data from Ref. 17. These data are from the midspan region of a linear cascade test, and are shown to illustrate the ability of the flow analysis to predict blade surface velocities. Blade surface velocities from the annular cascade data of Ref. 7 are shown in Fig. 2(b). The analytic curves show smaller radial variations over the last thirty percent of the chord for the contoured endwall than for the cylindrical endwall. The experimental and predicted radial variations in surface velocities over the latter part of the chord were about the same. The predicted profile loss was 0.021, and the endwall loss was 0.011. This resulted in an overall predicted loss of 0.032. The experimental results showed a loss of 0.022 in the midspan region, and an overall loss of 0.033.

Figure 3 shows predicted and measured flow angles. The experimental flow angle increased from

69.5° at 5 percent of span to 77.2° at 95 percent of span. The analytic variation was greater, showing greater flow turning near the tip. However, both the analysis and experimental data show significant spanwise variations in the flow angles. The analytic results are from the midchannel flow analysis (MERIDL code). At the measuring plane the flow analysis program TSONIC calculated a variation of a few degrees in the flow angle in the blade-to-blade direction. The local calculated midchannel flow angle was sensitive to the tolerance used to terminate the iteration for the downstream whirl. There was an uncertainty of about one degree in the local predicted flow angle.

Comparison With the Experimental Data of Ref. 10

The experimental results given in Ref. 10 are for two contoured stators and a cylindrical reference stator. Table I shows the three stator passage geometries. The cylindrical stator had a constant radius outer endwall. The conical stator had a variable radius outer endwall that decreased uniformly from inlet to exit. The S-contoured stator had a constant radius outer endwall in the front half of the passage, and an endwall defined by circular arcs in the rear half of the passage. The three stators were relatively small, having a tip diameter of 12.8 cm at the exit. The axial aspect ratio was 0.7 based on stator exit passage height, and the two contoured stators had an inlet to exit passage height ratio of 1.35. All three stators were lightly loaded, and Fig. 4 shows the blade loadings for the three stators at the design pressure ratio (inlet total to midspan exit static) of 1.8. Except at the tip, the surface velocities were similar for all three stators. At the hub and mean sections the surface velocities were slightly lower for the contoured cases. This was a result of the increased passage height for these geometries. When the S-contour geometry deflected the tip flow radiall inward, the surface velocities decreased. This was followed by a large overshoot in the suction surface velocity.

Flow Angles. Figures 5 and 6 show a comparison of the measured flow angles at two different pressure ratios. The analytic and experimental results are compared at a measuring plane one third of an axial chord downstream of the trailing edge. The analysis is able to predict the overturning of the flow for the contoured stators at both pressure ratios. There are two factors which might account for the difference in level between the experimental and analytic flow angles. The precision in measuring the flow angle was about one degree. As noted previously, there was an uncertainty of about one degree in the local predicted flow angle.

Loss Comparisons. Table II compares the predicted and experimental stator kinetic energy losses at three pressure ratios. Experimental data are shown at pressure ratios of 1.35, 1.8, and 1.95. As can be seen from Table II the analysis is able to predict the loss reduction due to contouring. However, it only predicts the level of stator loss to about 75 percent of the experimental value. This difference corresponded to 0.015 at design pressure ratio. Since the analysis only accounts for loss due to boundary layer growth and the presence of the trailing edge, but does not account for any losses due to secondary flows, it was expected that the analysis would underpredict the stator loss levels. Table II shows that about 40 percent of the predicted loss was due to endwall boundary layer growth. Because of the favorable pressure gradients within the passage most of this growth occurred between the trailing edge and the measuring plane. If the endwall boundary layer analysis were terminated at the trailing edge, the analysis would predict only about half of the measured loss.

The analysis predicted the level of loss better for the stator of Ref. 7 than for these stators. The stator of Ref. 7 had a larger aspect ratio, and endwall loss was a smaller fraction of total loss. An analytic investigation was done to see if maintaining continuity for the entire endwall sheet would change the predicted endwall loss for the stators of Ref. 10. This analysis used the boundary layer program of Ref. 18 (STAN5). The calculated loss using this program assuming isolated endwall streamlines gave the same results as the standard analysis using the BLAYER program of Ref. 13. When continuity was maintained for the endwall sheet, the calculated endwall loss increased from 0.017 to 0.019 for the cylindrical stator at design pressure ratio. Using this assumption resulted in a calculated total loss of 0.044 compared to a measured loss of 0.057. Accounting for continuity in the endwall boundary layer would change cylindrical and contoured endwall losses by the same amount, but would not change the improvement due to contouring.

In addition to reduced boundary layer growth it was expected that contouring would reduce losses associated with cross-channel or radial pressure gradients. For these tests it is seen from Table II that almost all of the experimental reduction in loss due to contouring is accounted for by the calculated reduction in loss due to reduced boundary layer growth. Since the cylindrical stator was lightly loaded (Fig. 4), there may not have been significant losses that were affected by reduced cross-channel or radial pressure gradients.

Reynolds Number Effect. Experimental data at different pressure ratios were obtained by varying the inlet pressure to maintain a fixed static pressure at the tip in the measuring plane. Because the level of loss increased with lower pressure ratios, an analytic investigation of the effect of Reynolds number on stator loss was undertaken. Boundary layer calculations were done for the three stators at the design pressure ratio. It was found that when the Reynolds number was increased by a factor of ten, the loss for the cylindrical stator was reduced from 0.042 to 0.032. At this higher Reynolds number the loss for the conical stator was reduced from 0.038 to 0.029, and for the S-contour stator the loss was reduced from 0.038 to 0.029. The loss associated with just the presence of the trailing edge was 0.010 for all three stator configurations, and was independent of Reynolds number. Since all calculations were done assuming turbulent flow, the variation of the transition location with Reynolds number did not enter into the calculations. These analytic results showed that the percent reduction in stator loss attributable to boundary layer growth for the two contoured stators was nearly constant over the range of Reynolds number investigated.

Height Ratio Effect. The experimental results in Table II show that both the full length conical stator and the S-contour stator had about the same improvement over the cylindrical stator. However, Ref. 9 showed that a full length contour has only half the improvement of a contour with the tip radius change in the rear half of the stator. The conclusions of Ref. 9 were drawn for a stator with a passage height ratio of 1.2. This reference also showed that there was little gain in loss reduction when the passage height ratio was increased beyond 1.2. The full-length conical contour with an actual passage height ratio of 1.35 can be viewed as a half-length contour with a passage height ratio of 1.18. When this is done the experimental data no longer contradict the analytic results of Ref. 9.

Radial Loss Distribution. Figure 7 shows contour plots of analytic local static to inlet total pressure ratios for the three stators at the design pressure ratio of 1.8. The lowest pressures are just in front of the trailing edge. The lowest pressures for the cylindrical stator are at the hub. For the S-contour stator there is a low pressure region a the tip. From these pressure contours it was expected that the loss would not be as great near the hub for the S-contour stator as for the cylindrical stator. This is verified experimentally. Figure 8 shows the experimental loss distribution as a function of passage height for the three stators. There was a high loss region near the hub for the cylindrical stator, while the loss was greater near the tip for both contoured stators. The two contoured stators had the same mass averaged loss, but the S-contoured stator had a higher loss region near the tip than the conical stator. The contour plots of Fig. 7 show the S-contour with a low pressure region near the tip, while the conical stator has little pressure variation from hub to tip. By comparison of Figs. 7 and 8 it appears that all that is required for the losses to be greater at the tip than at the hub is the absence of a low pressure region near the hub. From the results shown in Figs. 7 and 8 it may be possible to predict how the losses will be distributed radially using analytic static pressure contours. Improved stage performance is the primary goal, and whether the redistribution of stator loss helps or hurts stage performance is a function of stage geometry. There is evidence that the redistribution of loss can help significantly. Reference 2 showed an improvement in stage efficiency of 1.5 points with a contoured endwall, while the stator loss was reduced by only 0.002 with a contoured endwall.

Comparison With the Experimental Data of Ref. 8

Experimental results are given in Ref. 8 for three stators, and analytic comparisons were made for these tests. Three stators were tested, with two of them contoured. These stators had an exit tip diameter of 24 cm, about twice the size of the stators described in Ref. 10. Table I shows the passage geometry for the three stators. In these tests contouring occurred in the forward part of the blade, with the contour ending at about two-thirds of the axial chord. The two contoured geometries differed principally in the passage height ratio. The smaller one had a passage height ratio of 1.2, while the larger one had a passage height ratio of 1.3. The blade loadings for these stators are shown in Fig. 9 for a total inlet to mean static exit pressure ratio of 1.5. It can be seen that these stators were highly loaded, and that the loading differed considerably from the stators of Ref. 10. Figures 9(b) and (c) show a peak in the suction surface velocity in the region where the outer endwall changes radius. Reference 4 showed the same behavior for tests in a linear cascade.

Table III gives a comparison of the experimental and predicted stator loss for the three stators. Comparisons are made at the measuring plane, half a chord beyond the trailing edge. The analysis predicted the loss for the cylindrical case as only 0.045, while the measured loss was 0.084. The analysis was done assuming turbulent boundary layers. Even though there was a severe unfavorable pressure gradient in the front part of the blade (Fig. 9), no separation was predicted for the turbulent boundary layer. A laminar boundary layer would separate in the presence of this gradient. If it did reattach, it would reattach turbulent, and is more likely to reattach in the presence of a favorable pressure gradient. Figure 10(a) shows favorable velocity gradients in the rear part of the blade for the hub and mean suction surface velocity profiles. The tip section shows no favorable velocity gradient. Experimentally, the loss was very high near the tip for the cylindrical case. The flow may have separated in this region, and not reattached. If this occurred, the analysis did not recognize it, and greatly underpredicted the loss. The analysis predicted the loss level for the two contoured stators about as well as for the lightly loaded stators of Ref. 10. This is true even though the contoured stators of Ref. 8 were more highly loaded.

In an effort to determine if a different boundary layer analysis would show improved performance for the contoured stator, the calculated inviscid surface velocities for the cylindrical and small contour endwalls were used in the boundary layer analysis of Ref. 18 (STAN5). This analysis allows for boundary layer transition. When the boundary layer analysis was done, it was necessary to smooth the surface velocities. Nevertheless, there was a significant difference in the boundary layer results for the two cases. The boundary layer parameters for the contoured case did not change significantly from those calculated using the BLAYER program of Ref. 13, so that the calculated loss remained 0.044. However, the boundary layer growth was larger for the cylindrical case, resulting in a calculated loss of 0.050. According to the STAN5 boundary layer analysis of Ref. 18 the improvement in loss for the small contour was 0.006. The stator loadings of Refs. 8 and 10 were considerably different. The analysis predicted the losses for the three stators of Ref. 10 and the two contoured stators of Ref. 8 to about 75 percent of the experimental value at the same loss level. For these two stator designs it appears that loading does not cause additional loss other than what can be accounted for by boundary layer growth.

Evolution of a Contour Geometry. The experimental results of Ref. 8 showed that a contour could dramatically improve stator performance. The analysis indicated that placing the contour in the rear part of the passage could further increase stator performance. Figure 10 shows calculated blade loadings for different contour geometries using the stator geometry of Ref. 8. Calculations were done to define a contour which had reduced stator loss and no overturning at the tip. The flow angle at the tip for the cylindrical case was 72°. Figure 10(a) shows the blade velocities for a contour in the aft portion of the passage with a passage height ratio of 1.3. This contour showed a calculated loss reduction of 0.007 over the cylindrical endwall case, but the flow angle at the tip was 78°. Figure 10(b) shows the blade velocities when a passage height ratio of 1.2

was used. The calculated loss reduction was 0.006, but the flow angle at the tip remained 78°. Figure 10(c) shows the blade velocity profiles for a contour which changed over the entire passage length. The last quarter of the passage had the same contour as the one shown in Fig. 10(b) for a height ratio of 1.2. The height ratio was 1.3 at the leading edge, and the tip radius was faired in so that the front part mated with the contour in the rear quarter. This contour showed a loss reduction of 0.006, but the overturning at the tip has been reduced so that the flow angle was only 73°. One additional desirable feature of this contour was that the minimum surface pressures were the same at the hub and tip. The loss distribution is therefore expected to be similar to the loss distribution shown in Fig. 8 for the conical stator.

Concluding Remarks

Comparisons with experimental results have shown the ability of the quasi-three-dimensional analysis to predict the the change in stator performance when contoured endwalls are used. The analysis was able to predict the trends in flow angle variation resulting from the highly three-dimensional passage geometries. The improved stator performance is only part of the goal of overall stage improvement. The results of overall stage test, which are detailed enough to allow comparisons with analytic models, are eagerly awaited.

APPENDIX A - ANALYTIC MODEL FOR ENDWALL LOSS

The mass averaged kinetic energy loss at an axial location downstream of the stator was shown in Ref. 16 to be:

$$\overline{e} = 1 - \frac{\int_0^{\theta_p}\int_{r_h}^{r_t} \rho V^2 V_x r \, dr \, d\theta}{\int_0^{\theta_p}\int_{r_h}^{r_t} \rho V_i^2 V_x r \, dr \, d\theta} \tag{A-1}$$

This can be rearranged to give:

$$\overline{e} = \frac{\int_0^{\theta_p}\left[\int_{r_h}^{r_t} \rho V_i^2 V_x r \, dr - \int_{r_h}^{r_t} \rho V^2 V_x r \, dr\right] d\theta}{\int_0^{\theta_p}\int_{r_h}^{r_t} \rho V_i^2 V_x r \, dr \, d\theta} \tag{A-2}$$

Loss is assumed to occur only on the endwalls. Therefore, between $r_h + \delta_{fh}$ and $r_t - \delta_{ft}$, $V = V_{fs}$ and $V_i = V_{fs}$. It is assumed that the hub and tip boundary layers are thin relative to the span. Consequently, r is constant for each boundary layer. The axial velocity, V_x, is given by $V_x = V \cos \beta$. The flow angle, β, at each boundary is assumed to be the one determined from the inviscid flow analysis. The displacement thickness is given by:

$$\delta = \delta_f - \int_0^{\delta_f} \frac{\rho V}{\rho_{fs} V_{fs}} \, dr \tag{A-3}$$

The kinetic energy thickness is given by:

$$\psi = \int_0^{\delta_f}\left[1 - \left(\frac{V}{V_{fs}}\right)^2\right]\frac{\rho V}{\rho_{fs} V_{fs}} \, dr \tag{A-4}$$

After some algebra:

$$\overline{e} = \frac{\int_0^{\theta_p}\left[\left(\psi r \rho_{fs} V_{fs}^3 \cos \beta\right)_h + \left(\psi r \rho_{fs} V_{fs}^3 \cos \beta\right)_t\right] d\theta}{\int_0^{\theta_p}\left[\int_{r_h}^{r_t} \rho_{fs} V_{fs}^3 \cos \beta r \, dr - \left(\delta r \rho_{fs} V_{fs}^3 \cos \beta\right)_h - \left(\delta r \rho_{fs} V_{fs}^3 \cos \beta\right)_t\right] d\theta} \tag{A-5}$$

The local values for the boundary layer parameters are found from calculations assuming the flow follows the inviscid streamlines. The intergration in the pitchwise direction is done by Simpson's rule using results from the different streamlines.

SYMBOLS

r	radius
V	velocity
β	flow angle
δ_f	full boundary layer height
δ	displacement thickness
$\overline{e}$	kinetic energy loss coefficient
θ	pitchwise angle
θ_p	pitchwise distance for one passage
ρ	density
ψ	kinetic energy thickness

Subscripts:

cr	sonic condition
fs	freestream
h	hub
i	ideal
t	tip
x	axial direction

References

1. Deich, M. E. Zaryankin, A. E., Filippov, G. A., and Zatsepin, M. F., "Method of Increasing the Efficiency of Turbine Stages with Short Blades." Translation No. 2816, Associated Electrical Industries (Manchester) Limited, England, 1960.

2. Ewen, J. S., Huber, F. W., and Mitchell, J. P. "Investigation of the Aerodynamic Performance of Small Axial Turbines," ASME Paper 73-GT-3, Apr. 1973.

3. Morris, A. W. H.; and Hoare, R. G., "Secondary Loss Measurements in a Cascade of Turbine Blades with Meridional Wall Profiling," ASME Paper 75-WA/GT-13, Nov. 1975.

4. Kopper, F. C., Milano, R., and Vanco, M., "An Experimental Investigation of Endwall Profiling in a Turbine Vane Cascade," AIAA Paper 80-1089, July 1980.

5. Due, H. F.,Jr., Rogo, C., Kosier, C. L., and Jasas, G. B., "Advanced Small Axial Turbine Technology," USAAMRDL-TR-77-1, May 1977.

6. Okapuu, U., "Some Results from Tests on a High Work Axial Gas Generator Turbine," ASME Paper 74-GT-81, March 1974.

7. Timko, L. P. : Unpublished test memo of work done under contract NAS3-20643

8. Tipton, D. L., "Experimental Investigation of Turbine Endwall Contouring," Detroit Diesel Allison Rept. AX0400-174, Dec. 1981.

9. Boyle, R. J., Rohlik, H., and Goldman, L. J., "Analytic Investigation of Effect of End-wall Contouring On Stator Performance." NASA TP-1943, 1981

10. Haas, J. E., "Analytical and Experimental Investigation of Stator Endwall Contouring in a Small Axial-Flow Turbine - I. Stator Performance." NASA TP-2023, 1982.

11. Katsanis, T., and McNally, W. D., "Revised Fortran Program for Calulating Velocities and Streamlines on the Hub-Shroud Midchannel Stream Surface of an Axial-, Radial-, or Mixed-Flow Turbomachine or Annular Duct. Vol. I - User's Manual," NASA TN D-8430, 1977.

12. Katsanis, T., "Fortran Program for Calculating Transonic Velocities on a Blade-to-Blade Stream Surface of a Turbomachine," NASA TN D-5427, 1969.

13. McNally, W. D., "Fortran Program for Calculating Compressible Laminar and Turbulent Boundary Layers in Arbitrary Pressure Gradients," NASA TN D-5681, 1970.

14. Stewart, W. L., "Analysis of Two-Dimensional Compressible-Flow Loss Characteristics Downstream of Turbomachine Blade Rows in Terms of Basic Boundary-Layer Characteristics," NACA TN-3515, 1955.

15. Wood, J. R., "Improved Method for Calculating Transonic Velocities on Blade-to-Blade Stream Surfaces of a Turbomachine," NASA TP-1772, 1981.

16. Goldman, L. J., and McLallin, K. L., "Cold-Air Annular-Cascade Investigation of Aerodynamic Performance of Cooled Turbine Vanes. I - Facility Description and Base(Solid) Vane Performance," NASA TM X-3006, 1974.

17. Schwab, J. R., "Aerodynamic Performance of High Turning Core Turbine Vanes in a Two-Dimensional Cascade," AIAA Paper 82-1288, June 1982.

18. Crawford, M. E., and Kays, W. M., "STAN5 - A Program for Numerical Computation of Two-Dimensional Internal and External Boundary Layer Flows," NASA CR-2742, 1976.

Table I Description of experimental stators

	Source						
	Reference 7	Reference 10			Reference 8		
	Label						
	Contoured	Cylindrical	S-contour	Conical	Cylindrical	Small	Large
	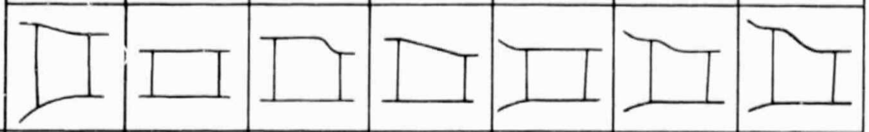						
Axial aspect ratio (at exit)	1.2	0.7	0.7	0.7	0.8	0.8	0.8
Inlet to exit passage height ratio	1.3	1.0	1.35	1.35	1.0	1.2	1.3
Tip diameter at exit, cm	73	13	13	13	24	24	24
Exit blade angle, deg	72	72	72	72	68	63	68
Mean axial exit solidity	.7	1.2	1.2	1.2	.6	.6	.6

Table II Comparison of predicted and measured loss for experiemntal data of Ref. 10.

Pressure ratio[a]		Kinetic energy loss		
		Stator		
		Cylindrical	Cone	S-Contour
1.35	Experimental Loss reduction	0.069 -----	0.061 .008	0.062 .007
	Predicted Profile Endwall Total Loss reduction	 0.030 .019 .049 -----	 0.026 .016 .042 .007	 0.026 .014 .040 .009
1.80 (Design)	Experimental Loss reduction	0.057 -----	0.052 .005	0.052 .005
	Predicted Profile Endwall Total Loss reduction	 0.025 .017 .042 -----	 0.023 .015 .038 .004	 0.024 .014 .038 .004
1.95	Experimental Loss reduction	0.057 -----	0.053 .004	0.053 .005
	Predicted Profile Endwall Total Loss reduction	 0.025 .017 .042 -----	 0.024 .014 .038 .004	 0.023 .013 .036 .006

[a]Inlet total to mean exit static.

Table III Comparison of predicted and measured loss for experimental data of Ref. 8.

Pressure ratio[a]		Kinetic energy loss		
		Stator		
		Cylindrical	Small contour	Large contour
1.5	Experimental Loss reduction	0.084 -----	0.060 .024	0.060 .024
	Predicted Profile Endwall Total Loss reduction	 0.020 .025 .045 -----	 0.019 .025 .044 .001	 0.019 .026 .045 .000

[a]Inlet total to mean exit static.

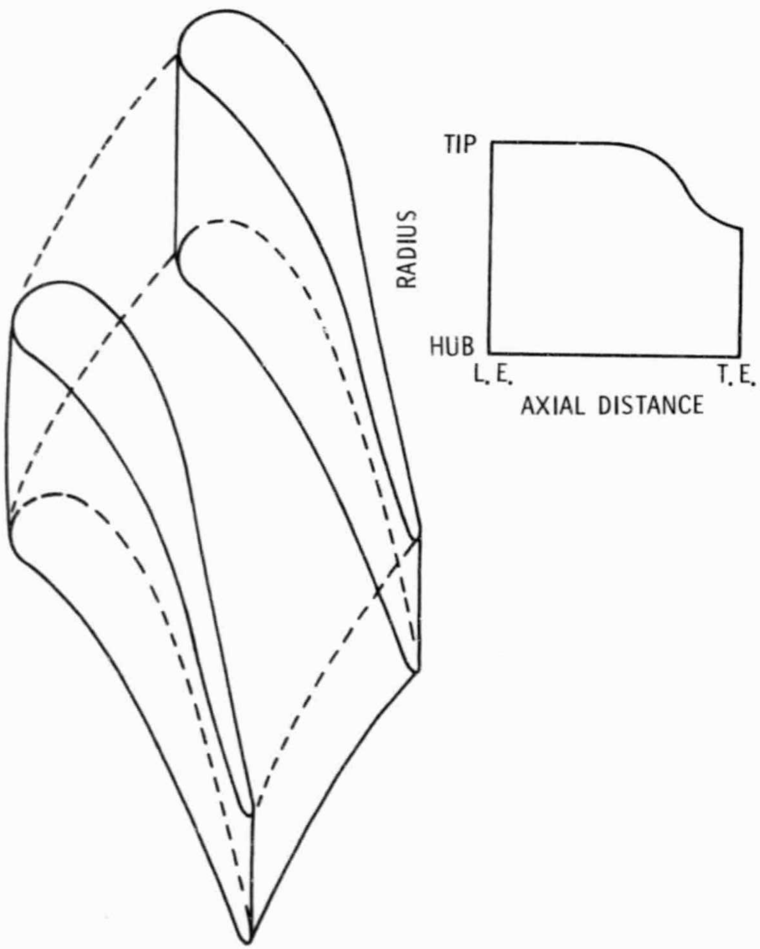

Figure 1. - Schematic of blade passage with a contoured tip.

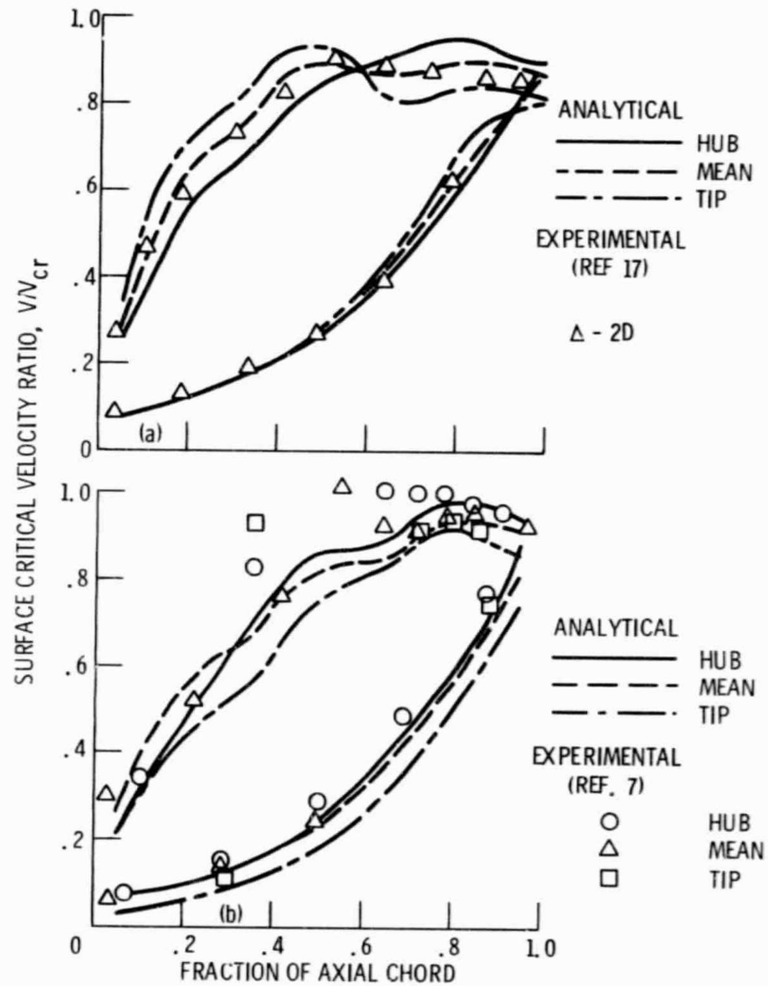

(a) Cylindrical stator.

(b) Contoured stator

Figure 2. - Suction and pressure surface velocities for cylindrical and contoured endwall stators.

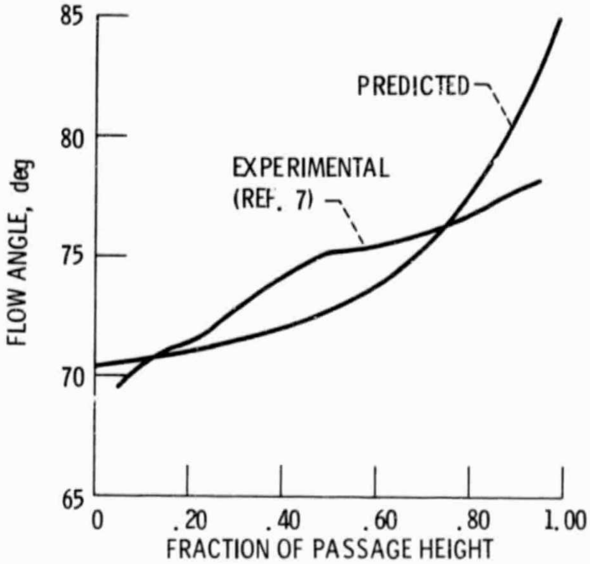

Figure 3. - Comparison of measured and predicted flow angles for experimental data of reference 7.

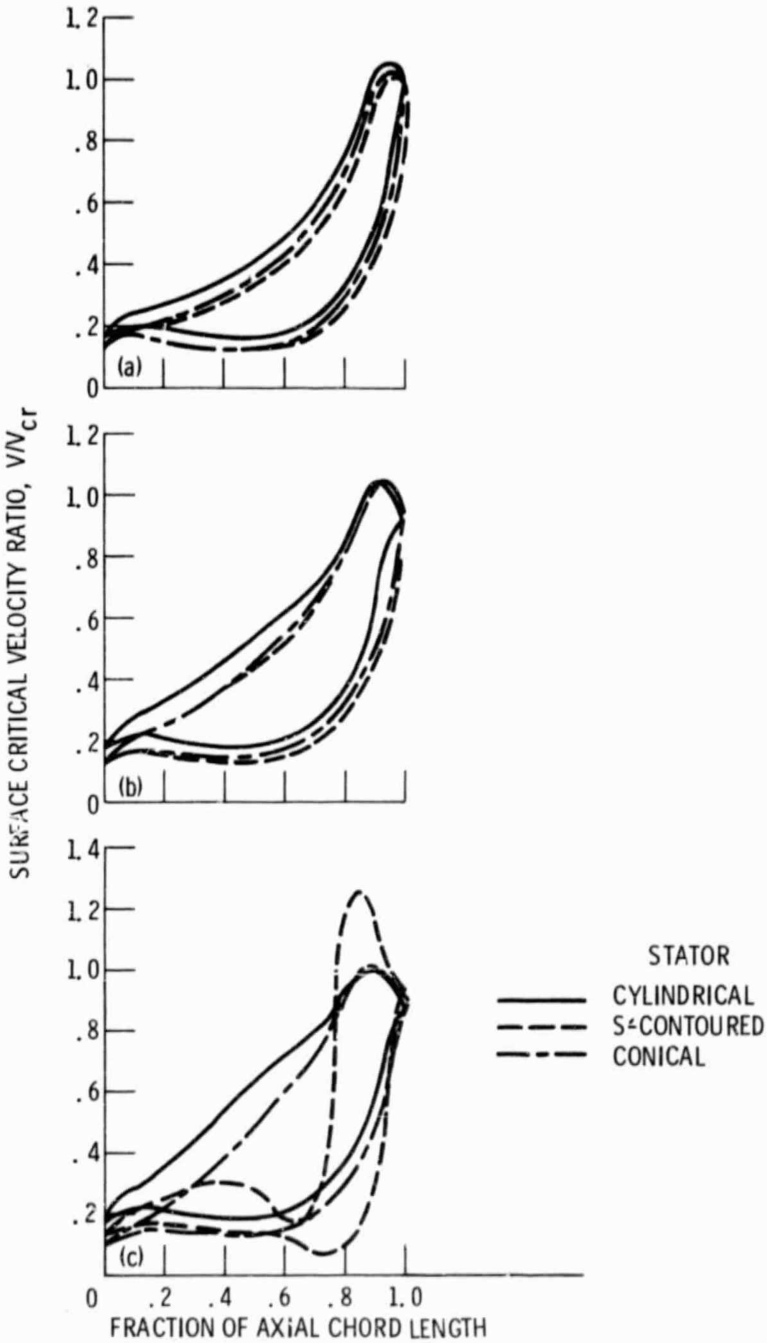

(a) Hub.

(b) Mean.

(c) Tip.

Figure 4. - Predicted blade surface velocities for cylindrical and contoured stators of reference 10, pressure ratio, 1.8.

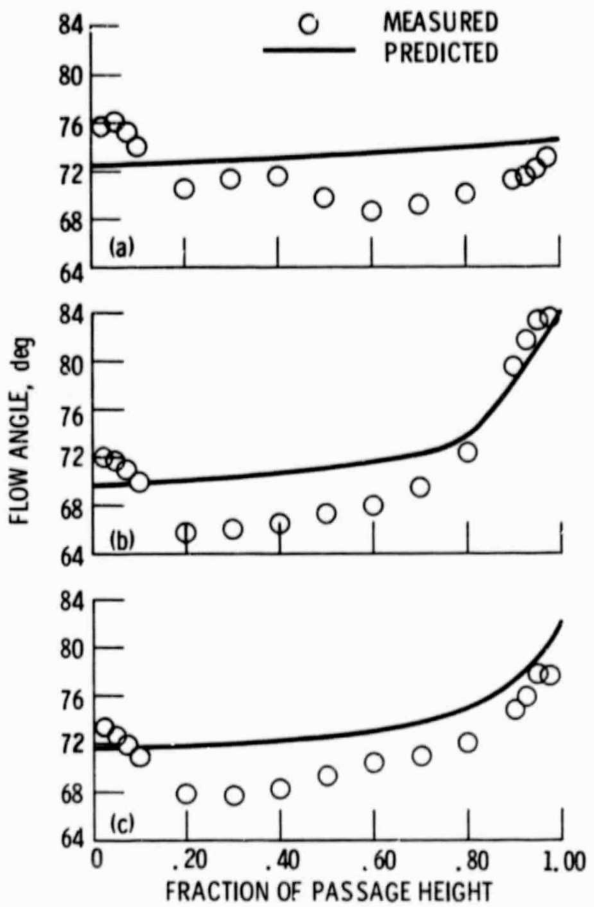

(a) Cylindrical stator.

(b) S-contoured stator.

(c) Conical stator.

Figure 5. - Comparison of predicted and measured flow angles for experimental data of reference 10. Inlet total to mean exit static pressure ratio, 1.35.

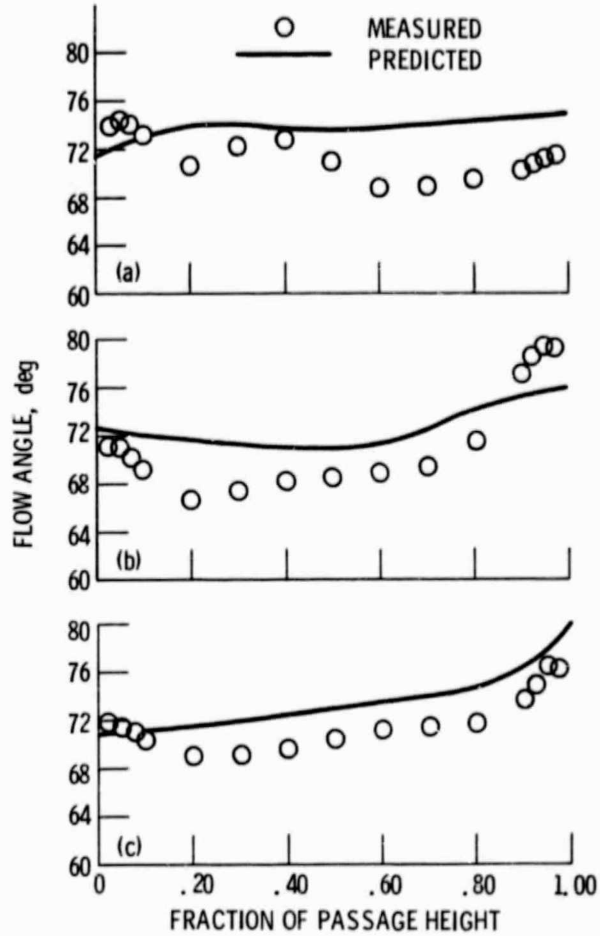

(a) Cylindrical stator.

(b) S-contoured stator.

(c) Conical stator

Figure 6. - Comparison of predicted and measured flow angles for experimental data of reference 10. Inlet total to mean exit static pressure ratio, 1.8.

ORIGINAL PAGE IS
OF POOR QUALITY

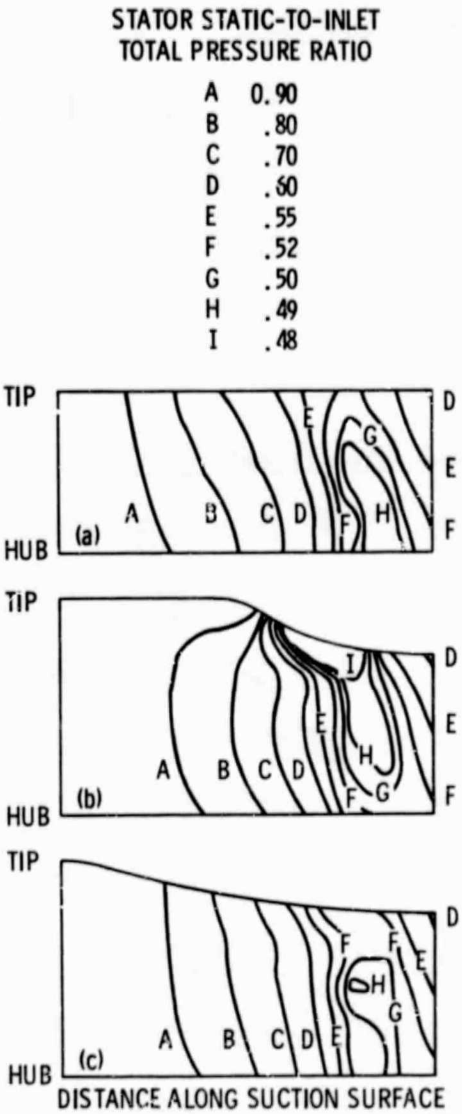

(a) Cylindrical stator.

(b) S-contoured stator.

(c) Conical stator.

Figure 7. - Analytic suction surface static pressure contours. Inlet total to mean exit static pressure ratio, 1.8.

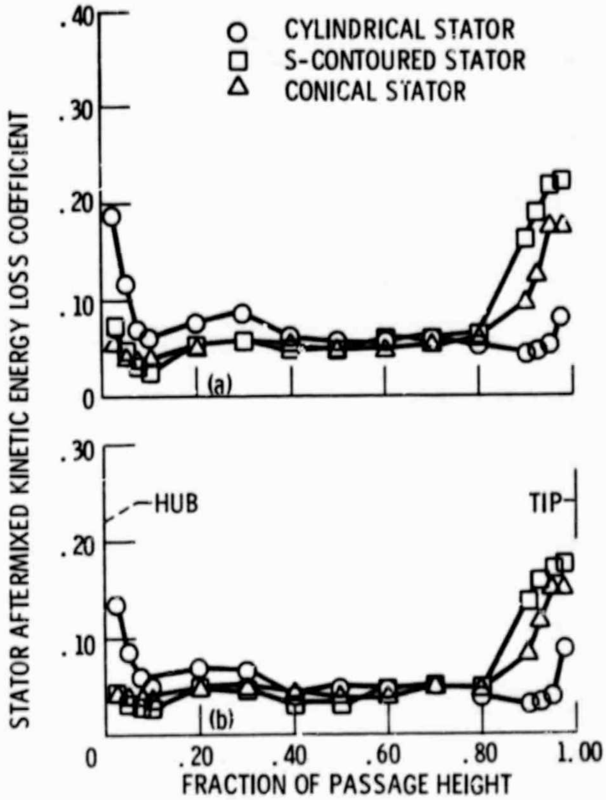

(a) Pressure ratio, 1.35.

(b) Pressure ratio, 1.8.

Figure 8. - Radial variation of stator experimental kinetic energy loss (from ref. 10).

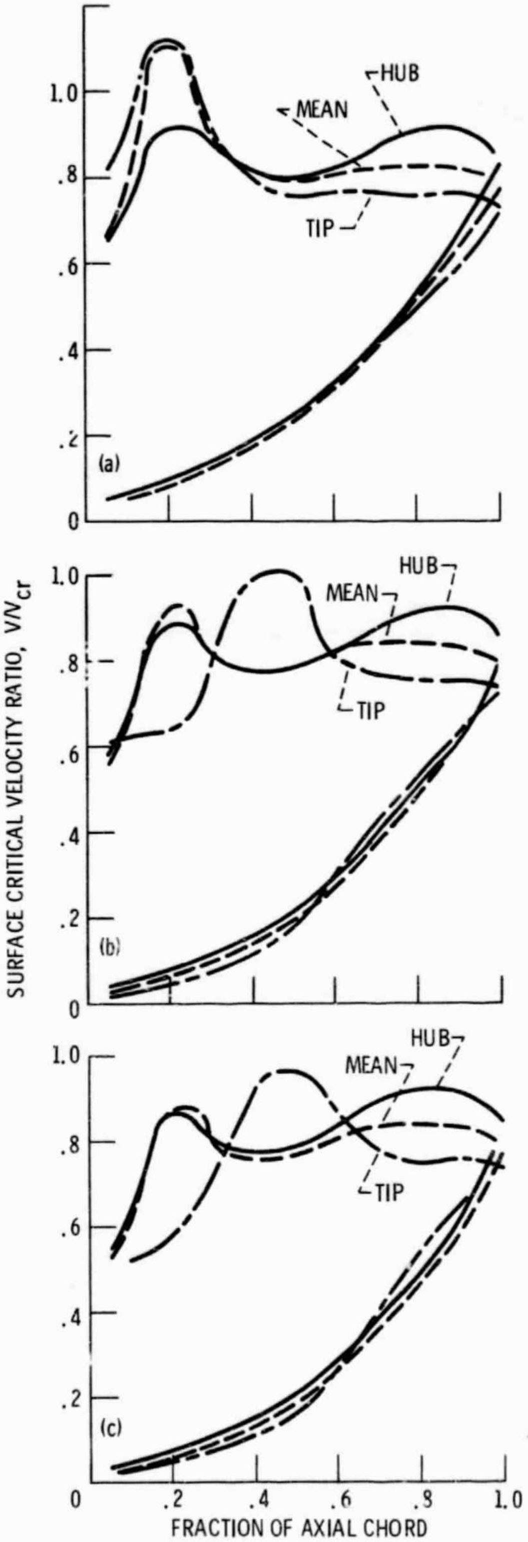

(a) Cylindrical tip.

(b) Small contour.

(c) Large contour.

Figure 9. - Surface velocities for three stators of reference 8.

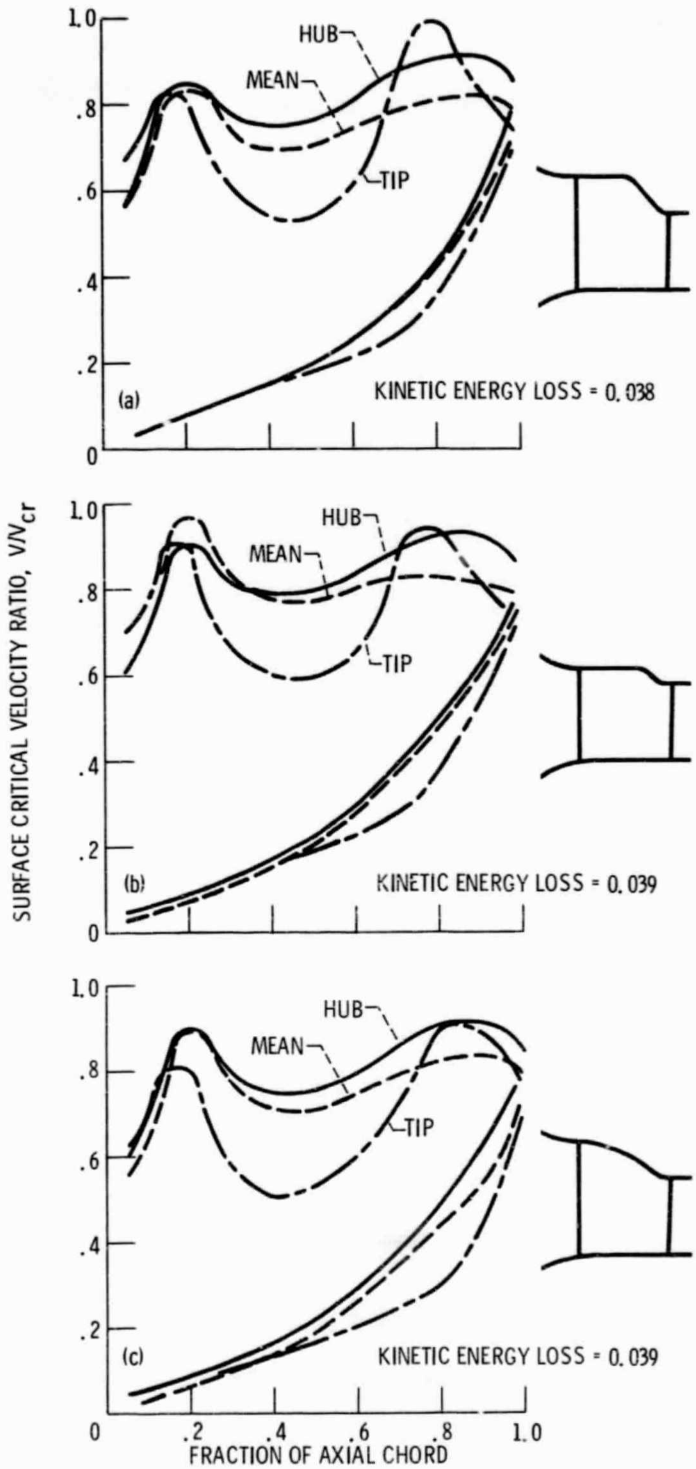

(a) Large contour at aft end.

(b) Small contour at aft end.

(c) Full length contour.

Figure 10. - Calculated pressure and suction surface velocities for different contour geometries.

1. Report No. NASA TM-82877 AVRADCOM TR-82-C-12	2. Government Accession No.	3. Recipient's Catalog No.
4. Title and Subtitle COMPARISON OF EXPERIMENTAL AND ANALYTIC PERFORMANCE FOR CONTOURED ENDWALL STATORS		5. Report Date 6. Performing Organization Code 505-32-2B
7. Author(s) Robert J. Boyle and Jeffrey E. Haas		8. Performing Organization Report No. E-1252 10. Work Unit No.
9. Performing Organization Name and Address NASA Lewis Research Center and AVRADCOM Research and Technology Laboratories Cleveland, Ohio 44135		11. Contract or Grant No. 13. Type of Report and Period Covered Technical Memorandum
12. Sponsoring Agency Name and Address National Aeronautics and Space Administration Washington, D. C. 20546 and U. S. Army Aviation Research and Development Command, St. Louis, Mo. 63166		14. Sponsoring Agency Code

15. Supplementary Notes
Robert J. Boyle, Lewis Research Center; Jeffrey E. Haas, Propulsion Laboratory, AVRADCOM Research and Technology Laboratories, Lewis Research Center, Cleveland, Ohio. Prepared for the Eighteenth Joint Propulsion Conference cosponsored by the AIAA, SAE, and ASME, Cleveland, Ohio, June 21-23, 1982.

16. Abstract
Comparisons between predicted and experimental stator losses showed that the analysis was able to predict the change in stator loss when contoured endwalls with highly three-dimensional passage geometry were used. The level of loss was predicted to within 75 percent of that measured. The predicted loss was due only to profile loss and boundary layer growth on the endwalls. The 25 percent difference was approximately 0.015 at design pressure ratio. The analysis was shown to predict the trend in stator flow angle, even for small stator geometries.

17. Key Words (Suggested by Author(s))	18. Distribution Statement
Stators Stator blades Turbomachinery	Unclassified - unlimited STAR Category 07

19. Security Classif. (of this report)	20. Security Classif. (of this page)	21. No. of Pages	22. Price*
Unclassified	Unclassified		

* For sale by the National Technical Information Service, Springfield, Virginia 22161